Cellular Physiology and Biochemistry

Cell Physiol Biochem 2018;49:1918-1932

DOI: 10.1159/000493653
Published online: 21 September, 2018

Accepted: 11 September, 2018







**Original Paper**

# Apelin-13 Administration Protects Against LPS-Induced Acute Lung Injury by Inhibiting NF-κB Pathway and NLRP3 Inflammasome Activation

Hailin Zhang[a] Sha Chen[b] Meichun Zeng[c] Daopeng Lin[a] Yu Wang[b] Xunhang Wen[a] Changfu Xu[a] Li Yang[d] Xiaofang Fan[b] Yongsheng Gong[b] Hongyu Zhang[e] Xiaoxia Kong[b]

[a]Department of Children's Respiration, The Second Affiliated Hospital & Yuying Children's Hospital, Wenzhou Medical University, Wenzhou, [b]School of Basic Medical Sciences, Institute of Hypoxia Research, Wenzhou Medical University, Wenzhou, [c]Department of Pathology, The First Affiliated Hospital, College of Medicine, Zhejiang University, Hangzhou, [d]Department of Respiratory Medicine, The First Affiliated Hospital of Wenzhou Medical University, Wenzhou, [e]School of Pharmaceutical Sciences, Wenzhou Medical University, Wenzhou, China

**Key Words**
Acute lung injury (ALI) • Lipopolysaccharide (LPS) • Apelin-13 • NF-κB • NLRP3

**Abstract**
***Background/Aims:*** Acute lung injury (ALI) is induced by a variety of external and internal factors and leads to acute progressive respiratory failure. Previous studies have shown that apelin-13 can decrease the acute lung injury induced by LPS, but the specific mechanism is unclear. Therefore, a mouse lung injury model and a cell model were designed to explore the mechanism of how apelin-13 alleviates the acute lung injury caused by LPS. ***Methods:*** The effect of apelin-13 on LPS-induced structural damage was determined by H&E staining and by the wet/dry weight ratio. The related inflammatory factors in BALF were examined by ELISA. The apoptotic pathway and the NF-κB and NLRP3 inflammasome pathways were evaluated by using Western blotting and immunofluorescence staining. ***Results:*** LPS induced the structural damage and the production of inflammatory cytokines in the lung tissues of mice. These deleterious effects were attenuated by apelin-13 administration. The protective effects of apelin-13 were associated with decreased reactive oxygen species (ROS) formation and the inhibition of the activation of the NF-κB and NLRP3 inflammasome pathways in mice and in Raw264.7 cells. ***Conclusion:*** Taken together, these data suggest that apelin-13 administration ameliorates LPS-induced acute lung injury by suppressing ROS formation, as well as by inhibiting the NF-κB pathway and the activation of the NLRP3 inflammasome in the lungs.



H. Zhang and S. Chen contributed equally to this work.

Xiaoxia Kong
and Hongyu Zhang

Institute of Hypoxia Research, Wenzhou Medical University
Wenzhou 325035, Zhejiang (China)
E-Mail kongxx@wmu.edu.cn; hyzhang@wmu.edu.cn

## Introduction

Acute lung injury (ALI), especially the severe form acute respiratory distress syndrome (ARDS), remains a major cause of morbidity and mortality in critically ill patients with ALI [1]. The pathogenesis of ALI/ARDS mainly involves exaggerated pulmonary inflammation, ultimately leading to an impairment of the alveolar-capillary barrier and to the deterioration of gas exchange [2, 3]. Lipopolysaccharide (LPS), a major biologically active component of the gram-negative bacterial cell wall, has long been widely used to induce pulmonary inflammation in a mouse model of ALI [4, 5]. As reported, injurious insults such as lipopolysaccharide (LPS) can activate reactive oxygen species (ROS), can cause the release of proteases for inflammatory mediator expression by activating the classic NF-κB signaling pathway and can induce the generation of inflammasomes [6-9]. A variety of molecular models of pathology or injury can trigger the activation of inflammatory bodies. After activation of the NLRP3 inflammasome, the cysteine protease caspase-1 is activated. Activated caspase-1 then begins to cleave the precursor forms of the pro-inflammatory cytokines IL-18 and IL-1β, which then mature and are secreted to ultimately participate in the corresponding inflammatory response [10-14]. When the organs cannot strictly regulate NLRP3 inflammasome activity, the body mounts a severe immune response, leading to excessive secretion of pro-inflammatory cytokines, which causes several physiological diseases such as autoimmune inflammation, tissue injury or chronic inflammation [15-18]. Therefore, maintaining the balance of pro- and anti-inflammatory factors and developing novel therapies to treat ALI and to improve clinical outcomes is urgently necessary.

The peptide apelin and the apelin receptor (APLNR) are present in the heart [13, 14] as well as the systemic and pulmonary vasculature (with the highest combined expression of these factors in lung tissue [19]), and they participate in the regulation of various physiological and pathological processes in the cardiovascular system, the digestive system, the endocrine system and the respiratory system [20-22]. Studies have shown that these peptides play an important role in endothelial protection, lipid antioxidation and the inhibition of neutrophil aggregation and activation, as well as having anti-inflammation and immunoregulatory effects [23-28]. In mouse models, treatment with apelin-13 ameliorates chronic normobaric hypoxia-induced anxiety-like behavior by down-regulating NF-κB activation [29]. It has been reported that NLRP3 inflammasome was significantly activated in hyperoxia-induced acute lung injury [30]. In severely burned rats, apelin inhibits the activation of the NLRP3 inflammasome, attenuates the systemic inflammatory response and promotes survival, in part through an endothelial nitric oxide synthase-dependent pathway [31]. In sepsis-induced cardiomyopathy, apelin-13 significantly reduced sepsis-induced cardiac impairment by decreasing the TLR4 and NLRP3 signaling-mediated inflammatory responses [32]. Our previous study found that apelin-13 had a biologically protective effect on lung injury induced by LPS. However, the protective mechanisms of apelin-13 are still unclear.

To study the function of apelin-13 in ALI, LPS was used to induce ALI in mice. Apelin-13 was then administered to mice with ALI, and the effects of the treatment on the NF-κB pathway and the NLRP3 inflammasome were evaluated.

## Materials and Methods

*Animal experiments*

All the animal study protocols were approved by the animal care and use committee of Wenzhou Medical College. Adult male C57BL/6N mice aged 8–10 weeks were randomly divided into 4 groups: the control group, the LPS (Sigma-Aldrich, L3129, LPS from *E. coli* 0127:B8) group, the apelin (Sigma Aldrich, USA)+LPS group and the apelin group. The mice in the apelin+LPS group and the apelin group were injected with apelin-13 at a dose of 10 nmol/kg 2 hours before LPS or saline administration. Next, the animals were treated once by an intratracheal instillation of 5 mg/kg of LPS in saline (or with saline as a control)

under anesthesia using chloral hydrate (Matrix, Orchard Park, NY, USA). After 6 hours of LPS instillation, bronchoalveolar lavage fluid (BAL fluid) and lung tissue were collected.

*Bronchoalveolar lavage fluid (BAL fluid)*

Bronchoalveolar lavage fluid was taken 6 hours after LPS administration. The mice in each group were anesthetized with an intraperitoneal injection of 5% chloral hydrate, and the thoracic cavity was exposed. Then, 0.8 ml of pre-cooled sterile PBS buffer was injected slowly through the total bronchial system into the lungs, resulting in a visual bulge in the lungs, and this pumping of buffer was repeated three times. The extracted lavage fluid was collected in an EP tube and was stored temporarily in the refrigerator at 4°C. The bronchoalveolar lavage fluid was centrifuged at 1, 500 r/min for 10 min. The supernatant was stored at -80°C, and the sediment was suspended in 1% BSA and placed on adhesive slides for immunofluorescence staining.

*Histology*

Biopsies of the lungs were fixed with 4% paraformaldehyde, were dehydrated, and were then embedded in paraffin. For the histological examination, the lung tissue samples were cut into 5 μm sections and were placed on glass slides. After deparaffinization and dehydration, the tissue samples were stained with hematoxylin and eosin (H&E). The stained slides were analyzed with a light microscope (Axio Imager M1, Karl Zeiss, Goettingen, Germany) under identical conditions. The sections were examined at 200× magnification for all the groups.

*Measurement of lung wet/dry weight ratio*

The lung wet/dry weight ratio was used to measure the water content in the lung tissue. Each lung was weighed before and after being dried in an 80°C oven for at least 24 hours until the weight was constant. The lung wet/dry ratio was calculated by dividing the wet weight by the dry weight of each lung.

*Enzyme-linked immunosorbent assay (ELISA)*

The expression of tumor necrosis factor (TNF)-α, interleukin (IL)-1β and IL-6 in the BAL fluid was measured using ELISA kits (e Bioscience Co., Ltd., CA, USA) according to the manufacturer's instructions. The levels were calculated using standard curves.

*Protein concentration in the BAL fluid*

The protein concentration in the BAL fluid supernatants was assessed using the BCA protein assay kit (Bio-Rad Laboratories). The measurement of the absorbance at 570 nm was performed with a microplate reader (Infinite 200, Tecan Group, Switzerland).

*ROS determination*

Reactive oxygen species (ROS) accumulation in the lungs was examined by dihydroethidium (DHE) staining. Cryostat lung sections were incubated with 5 μmol/L DHE (Molecular Probes, Eugene, OR) for 30 min at 37°C in the dark. The samples were then observed, and images were captured on a Nikon ECLIPSE Ti microscope (Nikon, Tokyo, Japan).

*Measurement of tissue and cell mitochondrial ROS production*

The mitochondria were isolated from tissue and cells using a mitochondria isolation kit (Wanleibio, China) following the manufacturer's instructions. The ROS production in the mitochondria was detected using the ROS-specific fluorescent probe DCFH-DA. The samples were incubated with 1 mM DCFH-DA at 37°C for 30 min. The fluorescence intensity was measured at 500 nm (excitation) and 525 nm (emission) using a fluorescence microplate reader.

*Western Blotting*

For the protein extractions, lung tissue or Raw264.7 cells were harvested and lysed in a protein extraction reagent (Pierce, Thermo Scientific) with a cocktail (Roche Life Science, Indianapolis, IN). The extractions of nuclear and cytoplasmic proteins from the lungs or cells were performed with nuclear and cytoplasmic protein extraction reagent kits (Beyotime Institute of Biotechnology). Protein concentrations

were determined using a BCA protein assay kit (Bio-Rad Laboratories). Equal amounts of protein from the samples were separated by SDS-PAGE on 10% or 12% denaturing gels at 120 V and were transferred onto polyvinylidene difluoride (PVDF) membranes (Bio-Rad Laboratories) at 300 mA for 90 min by the wet transfer method. The membranes were blocked in tris-buffered saline containing 5% skim milk for 2 h at room temperature. After three washes with 0.1% Tween-20 (TBST), the membranes were incubated with the specific primary antibodies against Bcl-2 (ab196495, 1:500-1:2, 000, abcam, USA), Bax (ab32503, 1:1, 000-1:10, 000, abcam, USA), Caspase-3 (#9664, 1:1, 000, CST, USA), I-κB (#4814S, 1:1, 000, CST, USA), p-IκB (#2859, 1:1, 000, CST, USA), NF-κB (SAB4502617, 1:500-1:1000, Sigma, USA), LaminB (ab16048, 1:1, 000, abcam, USA), NLRP3 (#15101, 1:1, 000, CST, USA), Caspase-1 (#2225, 1:1, 000, CST, USA), or IL-1β (#12426, 1:1, 000, CST, USA) overnight at 4°C. Following washing, the membranes were incubated with the relevant secondary antibodies (1:5, 000; Sigma) for 1 h at room temperature. The relative intensities of the bands were analyzed using an image analysis software program (ImageJ 1.44p, Wayne Rasband, National Institutes of Health, USA).

*Immunofluorescence staining*

Immunofluorescence staining was performed as described previously [31]. Briefly, 5 μm slices of the paraffin embedded sections of the lung tissue were prepared and baked in a 60°C constant-temperature oven for 60–120 min. After deparaffinization, antigen retrieval and serum blocking, the tissue samples were incubated with primary antibodies against NF-κB (Sigma, 1:200) or F4/80 (Abcam, 1:200) at 4°C overnight and were then incubated with the relevant secondary antibodies for 1 h at room temperature. The nuclei were stained with DAPI fluorescent dye for 5 min. All the images were captured on a Nikon ECLIPSE Ti microscope (Nikon, Tokyo, Japan), and the sections were examined at 400× magnification for all the groups.

*Cell culture and reagents*

The Raw264.7 cell line was purchased from the Cell Bank of the Chinese Academy of Sciences (Shanghai, China). The cells were cultured in DMEM medium supplemented with 10% fetal bovine serum (FBS) (GIBCO, USA), 100 IU/ml penicillin and 100 μg/ml streptomycin at 37°C with 5% $CO_2$ in air. Apelin-13 was dissolved in sterile saline at a concentration of 1 μmol/L and was carefully placed in each well with the prepared cells 1 hour before LPS treatment.

*CCK8 cell proliferation assay*

Raw264.7 cells were cultured in 96-well plates at a density of $1\times 10^4$ cells per well and were allowed to attach overnight. Cells were treated with LPS (0.05, 0.1, 0.5, 1, 5 and 10 μg/ml) for 24hr or 1 μg/ml LPS for different times (0, 3, 6, 12 and 24hr). Different concentration of apelin (0.1, 0.5, 1μmol/L) was added to Raw264.7 cells before LPS. Then volume of 10 μl Cell Counting Kit-8 solution (CCK8; Dojindo Laboratories, Japan) was added to each well, followed by 2 h of incubation. The absorbance of each well was measured at 450 nm using an automatic multiwell spectrophotometer.

*Measurement of the mitochondrial membrane potential (ΔΨm)*

The ΔΨm of the Raw264.7 cells was determined using the mitochondrial membrane potential assay kit with JC-1 (Beyotime, China). Briefly, Raw264.7 cells with different treatments were incubated with 10 μg/ ml JC-1 for 20 min at 37 °C and were then washed with washing buffer two times. All the images were captured on a Nikon ECLIPSE Ti microscope (Nikon, Tokyo, Japan).

*Statistical analysis*

The data are presented as the means ± SEM. The results for the animal experiments are representative of at least 3 independent experiments. Student's t-test was used for the statistical analysis of comparisons between two groups. For more than two groups, evaluation of the data was performed using a one-way analysis-of-variance (ANOVA) test, followed by Tukey's post-hoc test. $P$ values <0.05 were accepted as statistically significant.

## Results

*Apelin-13 decreases the structural damage and the production of inflammatory mediators in an LPS-induced lung injury mouse model*

To determine whether apelin-13 could protect against LPS-induced ALI, the histopathologic features of the lungs from the different groups were evaluated by light microscopy. Histological analyses showed marked infiltration of inflammatory cells into the alveolar space, peribronchial wall thickening, and vascular congestion in the lungs of the LPS-induced treated mice. These histologic changes were dramatically reduced by administration of apelin (Fig. 1A). To evaluate changes in lung edema, lung wet/dry weight ratios were measured. As shown in Fig. 1B, a notable increase in the lung wet/dry weight ratio was caused by LPS instillation compared with the control group ($p<0.05$). The wet/dry weight ratio was markedly attenuated by administration of apelin ($p<0.05$). A change in the total protein concentration in BALF is a characteristic of increased capillary permeability. A sharp increase in total protein in the BALF was observed in the LPS group ($p<0.01$), which was significantly blocked by apelin pretreatment ($p<0.01$) (Fig. 1C). Furthermore, the expression levels of the inflammatory factors TNF-α, IL-6 and IL-1β in the BAL fluid of the different groups were also measured by ELISA. Compared to the control group, the mice treated with LPS had significantly increased levels of the cytokines TNF-α (Fig. 1D, $p<0.01$), IL-6 (Fig. 1E, $p<0.01$) and IL-1β (Fig. 1F, $p<0.01$) in the BAL fluid, and administration of apelin-13 clearly attenuated these LPS-induced increases ($p < 0.05 \sim p < 0.01$). These results illustrated that administration of apelin-13 could alleviate LPS-induced lung injury in mice.

*Apelin-13 decreases reactive oxygen species (ROS) generation and mitochondrial apoptosis in LPS-induced mice*

To further evaluate the effects of apelin-13 on LPS-induced lung injury, the generation of reactive oxygen species in mice was assessed by DHE staining. As shown in Fig. 2A, stimulation with LPS significantly increased the ROS generation in the mouse lungs, which was largely reduced by apelin-13. We found consistent results in mitochondrial ROS production (Fig. 2B). Furthermore, the protein expression levels of B-cell lymphoma 2 (Bcl-2), Bcl-2 X-associated protein (Bax) and cleaved caspase-3 were measured by Western blotting. Our results showed that LPS significantly increased the expression levels of Bax and cleaved caspase-3 ($p < 0.01$) and decreased the expression level of Bcl-2 ($p < 0.05$). These effects were markedly reversed by treatment with apelin (Fig. 2C-E, $p < 0.05 \sim p < 0.01$). These results indicated that apelin-13 alleviated oxidative stress and mitochondria-mediated cell apoptosis induced by LPS in mice.

*Apelin-13 prevents the nuclear translocation of NF-κB in LPS-treated mice*

To assess the effects of apelin-13 on the NF-κB inflammatory pathway, the expression of classic IκB/NF-κB pathway proteins were measured *in vivo* by Western blotting. As shown in Fig. 3A and 3B, the cytosolic level of *p*-IκBα was rapidly activated in mice treated with LPS for 6 h ($p<0.01$), and LPS administration caused the nuclear translocation of NF-κB p65 in the injured lungs of mice with ALI ($p<0.01$). Both of these phenotypes were significantly inhibited by pretreatment with apelin-13 ($p<0.05\sim p<0.01$). Furthermore, we investigated whether macrophages could be involved in ALI induced by LPS using immunofluorescence staining for F4/80 (a mouse macrophage-specific marker). As shown in Fig. 3C, LPS injection enhanced F4/80 immunoreactivity in the lung tissue, indicating increased macrophages infiltration; however, apelin-13 administration markedly reduced macrophage infiltration. These results indicated that apelin-13 inhibited the nuclear translocation of NF-κB p65 and the macrophage infiltration induced by LPS in mice.

*Apelin-13 inhibits the NLRP3 inflammasome inflammatory pathway in LPS-treated mice*

To assess the effects of apelin on LPS-induced NLRP3 inflammasome activation, the expression of the inflammatory cytokines NLRP3, caspase-1 and IL-1β were examined in

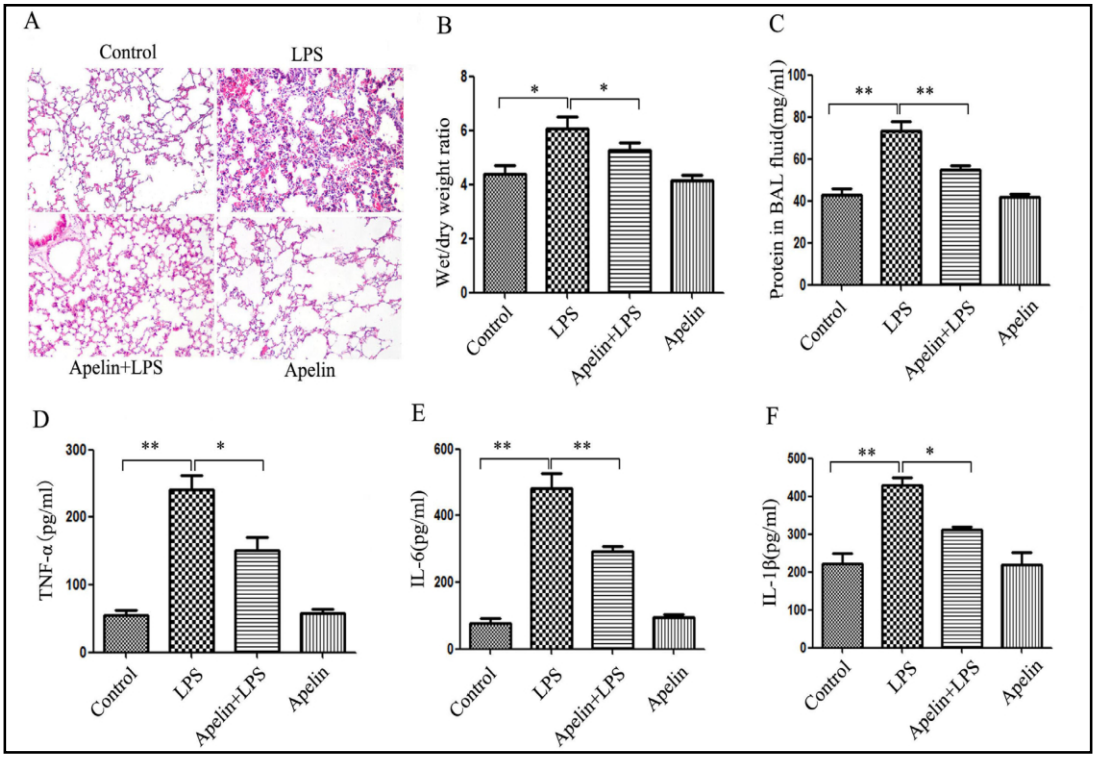


**Fig. 1.** Apelin-13 decreases the structural damage and the production of inflammatory mediators in LPS-induced lung injury mouse model. (A) Pathological changes in the lung tissues observed by H&E staining (200×). (B) The lung weight/dry weight ratio (W/D) was assessed among experimental groups. (C) Total protein level in BAL fluid (n=6). The levels of TNF-α (D), IL-6 (E) and IL-1β (F) in BALF were detected by ELISA. The data are presented as the mean ± SEM, from 3 independent experiments. * represented p<0.05; ** represented p<0.01.

the different groups by Western blotting. The results showed that the expression levels of NLRP3 (Fig. 4A, $p<0.01$), cleaved caspase-1 (Fig. 4B, $p<0.05$) and IL-1β (Fig. 4C, $p<0.01$) were significantly increased in the LPS group compared with the control group, while apelin-13 markedly reduced the expression of all three inflammatory cytokines (Fig. 3E, $p<0.05$~ $p<0.01$). These results indicated that apelin-13 inhibited the activation of the NLRP3 inflammasome induced by LPS in lung tissue.

*Apelin-13 protects Raw264.7 cells from injury induced by LPS*

To mimic LPS-induced lung injury, the effects of LPS on the viability of Raw264.7 cells was determined using the CCK8 assay. As shown in Fig. 5, treatment of the cells with LPS at 0.05, 0.1 and 0.5 μg/ml did not affect cell viability ($p > 0.05$) (Fig. 5A), whereas cell viability was significantly decreased after treatment with LPS at concentrations of 1, 5 and 10 μg/ml ($p<0.05$~ $p<0.01$). At the same time, treatment of the cells with 1 μg/ml of LPS resulted in obvious decreases in cell viability at 6, 12 and 24 h (Fig. 5B). Therefore, we chose 1 μg/ml LPS for 6 h for further experiments. The CCK8 assay also showed that the decrease in viability after 6 h of LPS stimulation was rescued in the cells pre-treated with 1μmol/L apelin-13 ($p< 0.05$). Apelin-13 alone had no significant effect on cell viability (Fig. 5C). Therefore, 1μmol/L apelin-13 was chose for following experiments. To explore the possible mechanism involved in the reversal of acute lung injury, the levels of apoptosis in Raw264.7 cells were determined by Western blotting, and the effect of apelin-13 on the mitochondrial membrane potential was detected by JC-1 staining. As shown in Fig. 5D, LPS significantly induced the loss of mitochondrial membrane potential, which was markedly reversed by treatment with apelin-13. Mitochondrial dysfunction may trigger the release of large amounts of ROS. Our

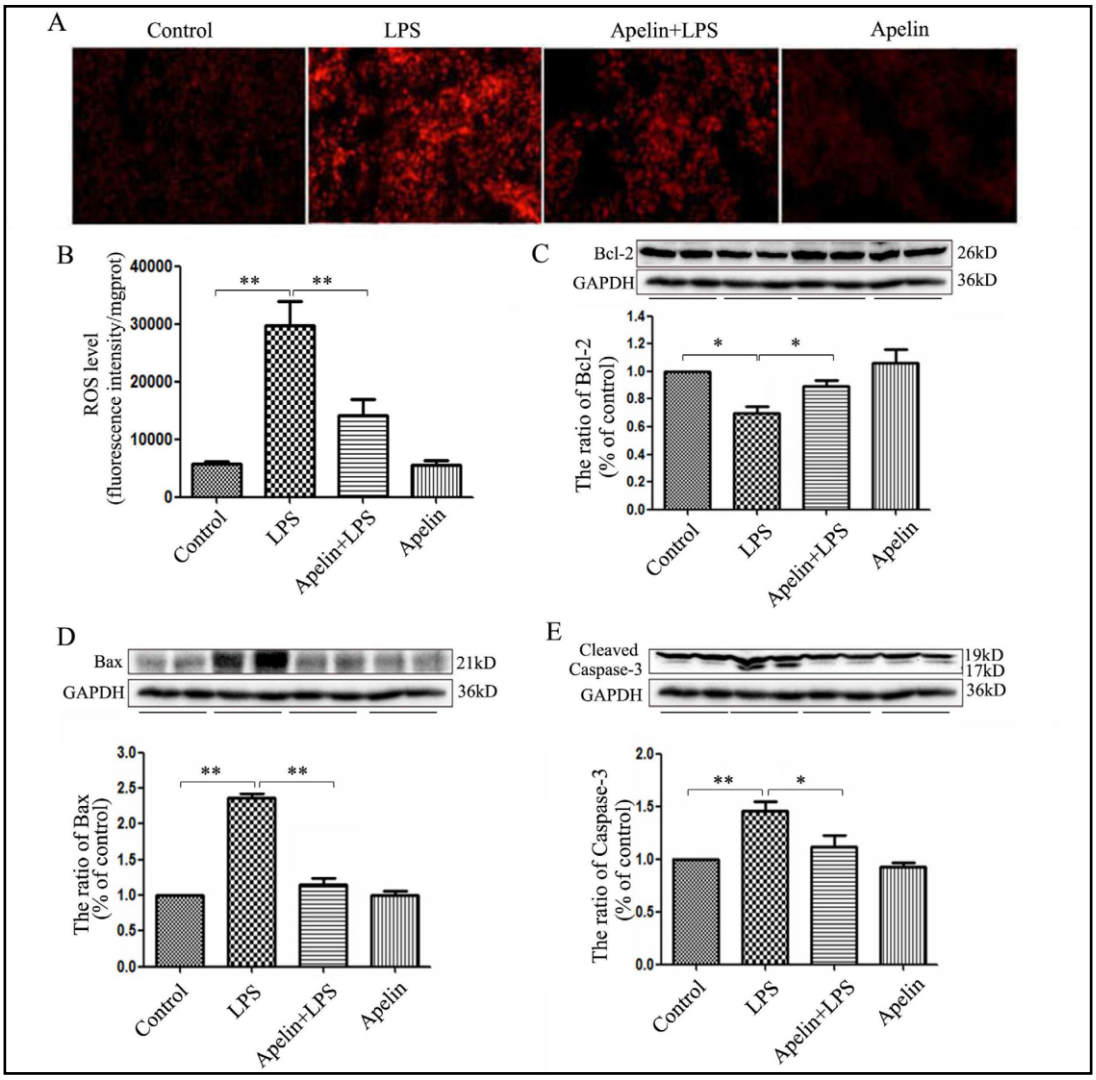


**Fig. 2.** Apelin-13 decreases ROS and mitochondrial apoptosis in LPS-treated mice. (A) ROS level in the lung tissues were observed by DHE staining (red, 400×). (B) The levels of ROS were assessed by fluorescence microplate reader. The protein expression levels of Bcl-2(C), Bax(D), Caspase-3(E) in lung extracts were detected by Western blotting. The data are presented as the mean ± SEM(n=6), from 3 independent experiments. * represented p<0.05; ** represented p<0.01.

results demonstrated that apelin blocked the increase in ROS levels induced by LPS (Fig. 5E, $p<0.01$). Furthermore, we evaluated the activation status of Bcl-2, Bax and cleaved caspase-3. As shown in Fig. 5F-H, LPS markedly increased the expression levels of Bax ($p<0.01$) and cleaved caspase-3 ($p<0.01$) and decreased the level of Bcl-2 ($p<0.01$), and these changes were significantly reversed by apelin ($p<0.05 \sim p<0.01$). These results indicated that apelin-13 inhibited the cell injury and apoptosis induced by LPS in Raw264.7 cells.

*Apelin-13 attenuates the nuclear translocation of NF-κB p65 induced by LPS in Raw264.7 cells*

The effects of apelin-13 on NF-κB activation on LPS-induced Raw264.7 cell injury was further investigated. The expression levels of proteins in the classic NF-κB pathway in Raw264.7 cells were examined. The results of Western blotting and immunofluorescence staining indicated that compared with the control group, the levels of p-IκB and nuclear-localized NF-κB p65 clearly increased after LPS administration in Raw264.7 cells ($p< 0.01$).

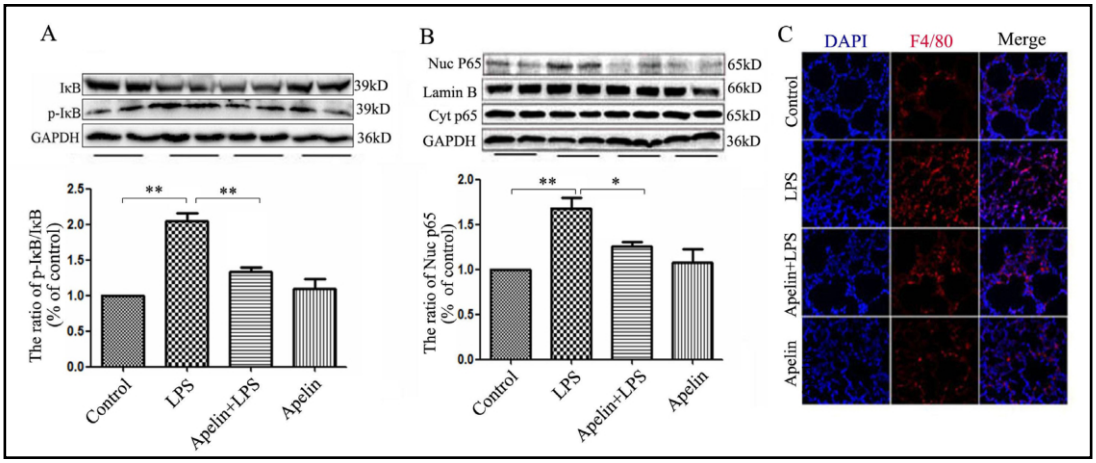


**Fig. 3.** Apelin-13 prevents the nuclear translocation of NF-κB in LPS-treated mice. (A) The protein expression levels of IκB and p-IκB in lung extracts. (B) The protein expression levels of nucleus p65 and cytoplasm p65 in lung extracts. (C) Macrophages infiltration was detected by F4/80 staining. The data are presented as the mean ± SEM(n=6), from 3 independent experiments. * represented p<0.05; ** represented p<0.01.

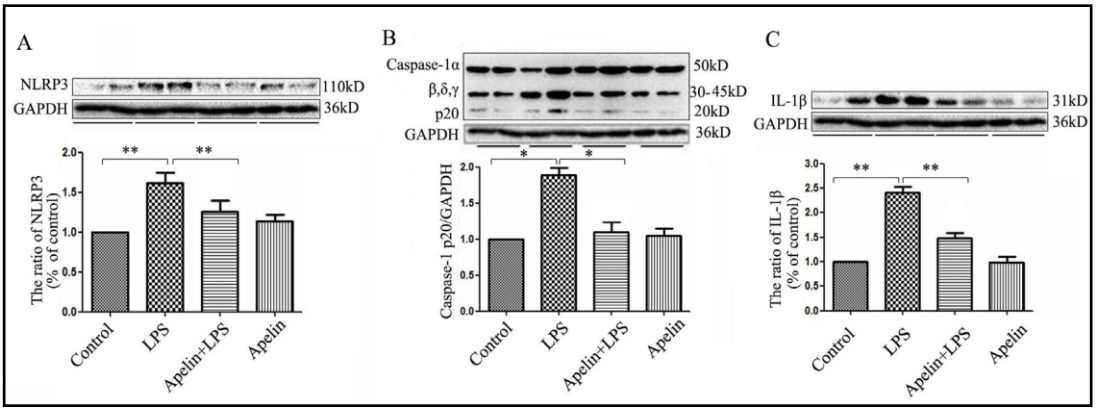


**Fig. 4.** Effect of apelin-13 on activation of NLRP3 inflammasome induced by LPS. The protein expression levels of NLRP3 (A), Caspase-1(B) and IL-1β(C) in lung extracts. The data are presented as the mean ± SEM(n=6), from 3 independent experiments. * represented p<0.05; ** represented p<0.01.

However, pretreatment with apelin-13 clearly blocked the increased expression of p-IκB and the nuclear translocation of NF-κB p65 induced by LPS ($p$< 0.01) (Fig. 6A-C). These results indicated that apelin-13 inhibited the induction of the NF-κB inflammatory pathway by LPS in Raw264.7 cells.

*Apelin-13 inhibits the induction of the NLRP3 inflammatory pathway by LPS in Raw264.7 cells*

The expression levels of proteins involved in the NLRP3 inflammatory pathway in Raw264.7 cells were detected by Western blotting. The results showed that LPS treatment significantly increased the levels of NLRP3 ($p$< 0.01) (Fig. 7A) and activated caspase-1 ($p$< 0.01) (Fig. 7B), as well as contributed to IL-1β maturation ($p$< 0.05) (Fig. 7C), and all of these effects were reversed by apelin-13 ($p$< 0.05~$p$< 0.01). Moreover, consistent with the Western blotting results, ELISA assays showed that apelin inhibited IL-1β secretion induced by LPS ($p$< 0.01) (Fig. 7D). These results indicated that apelin-13 attenuated the injury of LPS-induced Raw264.7 cells by inhibiting the NLRP3 inflammatory pathway.

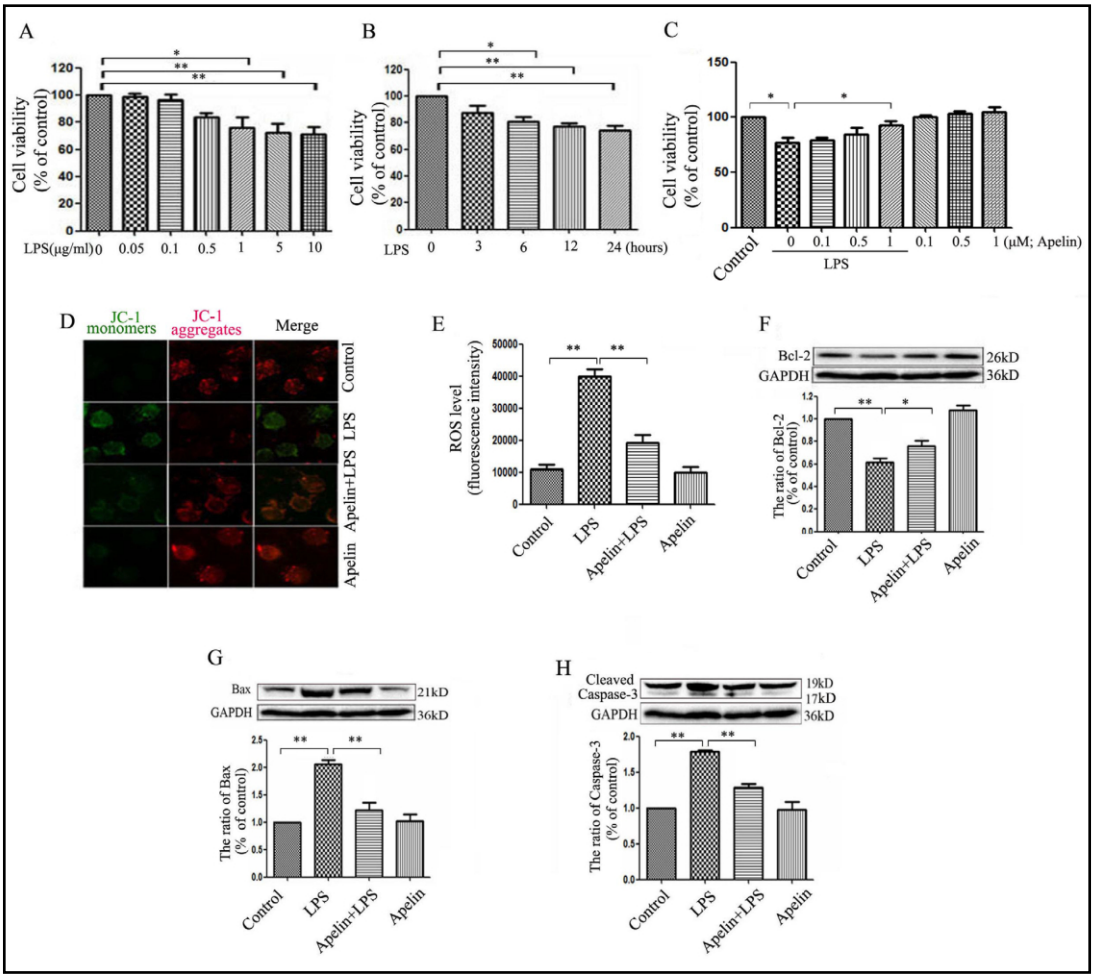


**Fig. 5.** Apelin-13 protects Raw264.7 cells injury induced by LPS. (A) Cell viability in different LPS concentrations (0.05, 0.1, 0.5, 1, 5 and 10μg/ml) for 24h was measured by CCK8 in Raw264.7 cells. (B) Cell viability for different times (0, 3, 6, 12 and 24h) at LPS 1 μg/ml was measured by CCK8. (C) Cell viability in different group was detected by CCK8 assay. (D) The mitochondrial membrane potential changes in Raw264.7 cells observed by JC-1 staining (JC-1 monomers is green and JC-1 aggregates is red). (E) The levels of ROS were assessed by DCFH-DA. The protein expression levels of Bcl-2 (F), Bax (G) and Caspase-3 (H) in Raw 264.7 cells extracts. The data are presented as the mean ± SEM(n=5), from 3 independent experiments. * represented $p<0.05$; ** represented $p<0.01$.

## Discussion

Our study provides some new information about the roles of apelin in LPS-induced acute lung injury *in vivo* and *in vitro*. Although, in our previous study, we found that apelin restrains lung injury induced by LPS, the underlying molecular mechanisms were not entirely clear. In the present study, we further demonstrated that treatment with apelin reduced LPS-induced oxidative damage, apoptosis and inflammatory responses, providing additional evidence that apelin might serve as a protective drug for LPS-induced acute lung injury.

ALI remains a severe disease that threatens human life around the world and manifests as abnormal gas exchange or chest pain. Despite the development of innovative therapies and intensive care, ALI induced by bacteria or other microbial infection remains an unresolved issue. The peptide apelin is a recently described ligand for the G-protein-coupled receptor APJ (APLNR) [22]. Apelin is closely linked to the occurrence and development of ARDS, pulmonary hypertension, lung cancer and other respiratory diseases [24, 33, 34]. It has been shown that apelin has a

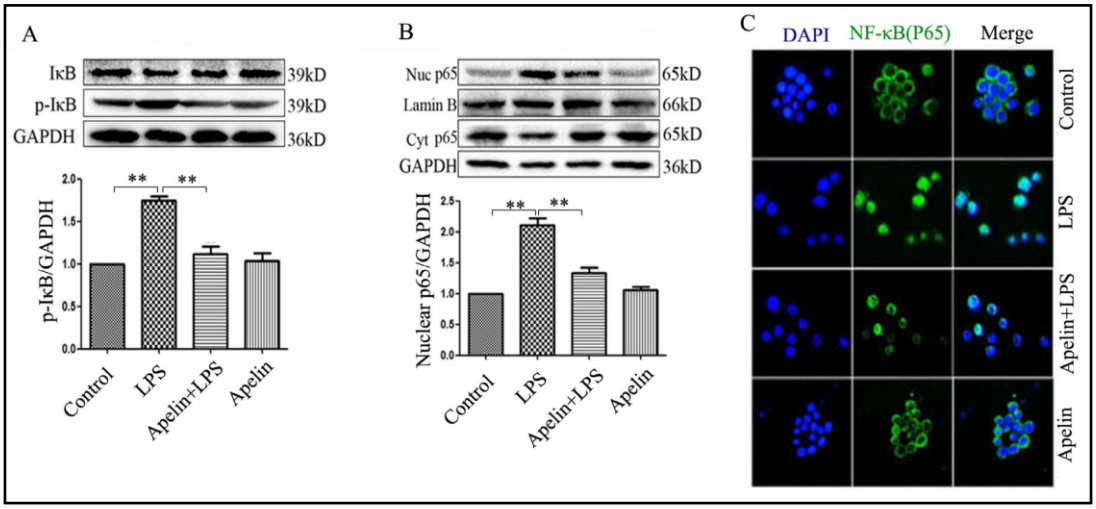


**Fig. 6.** Apelin-13 attenuates the nuclear translocation of NF-κB p65 induced by LPS in Raw264.7 cells. (A) The protein expression levels of IκB and p-IκB in Raw264.7 cells extracts. (B) The protein expression levels of nucleus p65 and cytoplasm p65 in Raw264.7 cells were detected by Western blotting. (C) Nuclear translocation of protein NF-κB p65 (green, 400×) in Raw264.7 cells observed by immunofluorescence staining. The data are presented as the mean ± SEM (n=5), from 3 independent experiments. * represented $p<0.05$; ** represented $p<0.01$.

positive inotropic effect on normal and injured myocardia in rats [35, 36]. At the same time, the apelin-APJ system has the potential to compensate for cardiac function, and a decrease in its expression and function is a possible reason for the occurrence and development of heart failure [34, 35, 37]. In our previous study, apelin-13 treatment significantly alleviated lung inflammation and injury and improved oxygenation in OA- and LPS-induced lung injury [38]. Our data showed that LPS stimulation significantly induced lung tissue histological changes and increased the expression of inflammatory cytokines and the total protein content in bronchoalveolar lavage fluid, as well as other indicators of change, indicating that these mice showed obvious characteristics of ALI/ARDS. When exogenous apelin-13 was given, the pathological changes and the expression of the inflammatory cytokines TNF-α, IL-6 and IL-1β in the bronchoalveolar lavage fluid significantly decreased. In addition, apelin-13 significantly attenuated lung wet/dry weight ratios and protein leakage in BALF. These findings indicated the potential therapeutic effects of apelin-13. Furthermore, we explored the underlying mechanisms of apelin-13-mediated protection against LPS-induced lung injury.

Oxidative stress characterized by excessive ROS is central to the severe pulmonary inflammation that results in ALI/ARDS [39]. It is reported that apelin can inhibit apoptosis in the ischemic myocardium by up-regulating Bcl-2 expression and by down-regulating Bax and cleaved caspase-3 [40] and that it can also reduce the damage to myocardial cells induced by ischemia reperfusion by activating the PI3k/akt pathway in isolated rat hearts [41]; it can also prevent reactive oxygen-dependent cardiac hypertrophy [42]. Our results were consistent with previous studies and showed that LPS induced a significant decrease in ΔΨm and an increase in ROS levels in lung tissue, which could be reversed by apelin-13 treatment. Moreover, we demonstrated that LPS clearly up-regulated the levels of the pro-apoptotic protein Bax and cleaved caspase-3 and down-regulated the level of the anti-apoptotic protein Bcl-2 in lung tissue and in Raw264.7 cells and that these effects could be reversed by apelin-13 treatment. Therefore, apelin exerted protective effects by eliminating the ROS and the mitochondria damage induced by LPS stimulation in mice.

Inflammatory cell infiltration and pro-inflammatory cytokine generation are both important characteristics in the process of LPS-induced ALI [43, 44]. ROS generation is a crucial regulator of modifications of inflammatory pathways during acute inflammation of

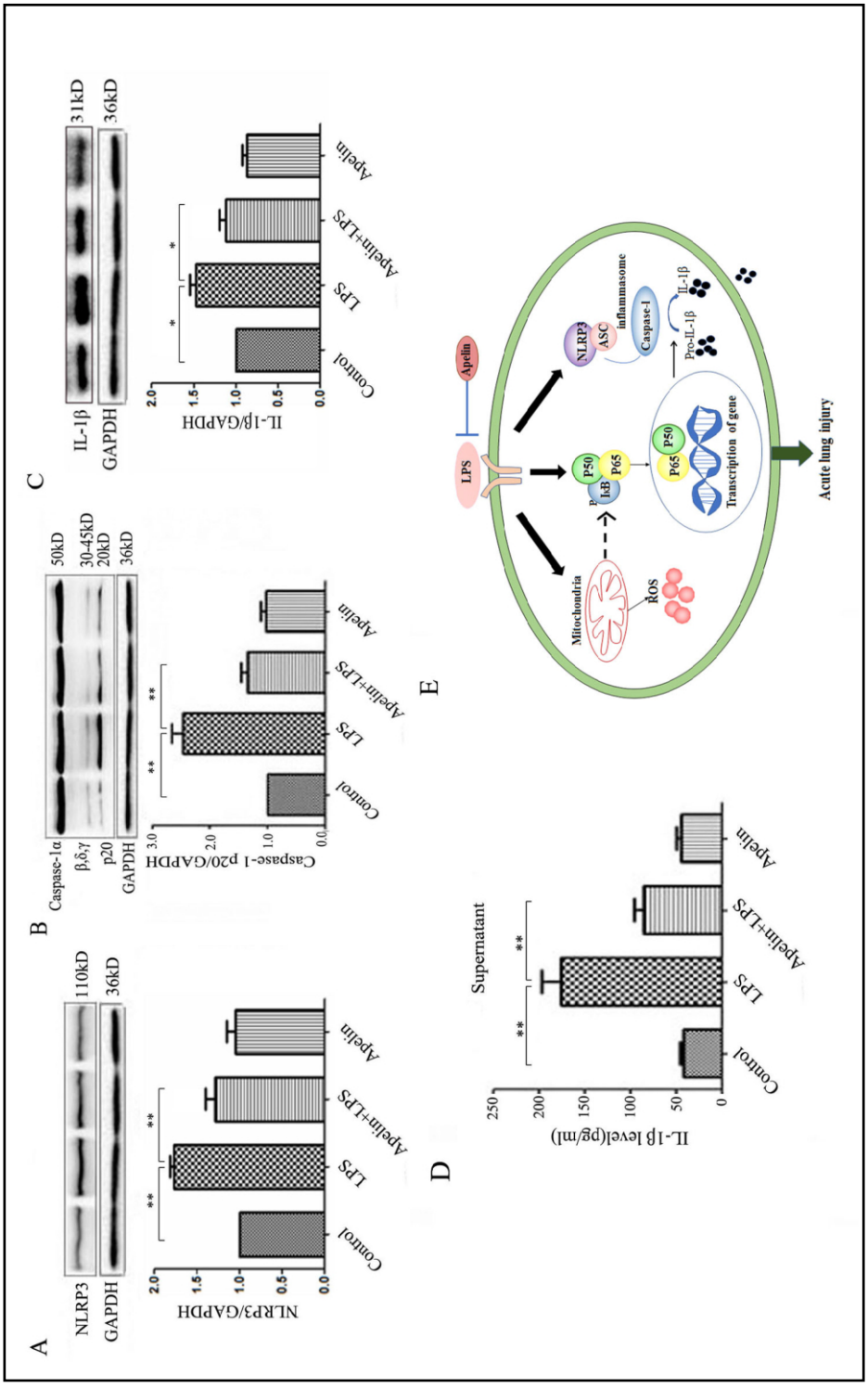


**Fig. 7.** Apelin-13 inhibits NLRP3 inflammatory pathway induced by LPS in Raw264.7 cells. The protein expression levels of NLRP3(A), Caspase-1(B) and IL-1β(C) in Raw264.7 cells were detected by Western blot. (D) The level of IL-1β in supernatant was detected by ELISA. (E) Illustration of protection provided by apelin against LPS-induced lung injury. The data are presented as the mean ± SEM (n=5), from 3 independent experiments. * represented p<0.05; ** represented p<0.01.

the lungs [45]. It has been reported that LPS treatment can activate ROS and can further stimulate NF-κB signaling, and these results are consistent with our previous studies [6, 46]. In the study of Lu et al., in human umbilical vein endothelial cells, apelin-APJ induced ICAM-1, VCAM-1 and MCP-1 expression via the NF-κB/JNK signaling pathway [47]. In our model, administration of apelin-13 inhibited the classic NF-κB signaling pathway and the activation of NF-κB, and it limited macrophage infiltration induced by LPS *in vivo* and in Raw264.7 cells.

The results also indicated that strict regulation of the activity of NLRP3 inflammatory bodies is an important part of maintaining immune homeostasis. A large number of studies have shown that the activation of the NLRP3 inflammatory body can induce severe autoimmune disease. *In vivo* evidence also indicated that LPS can activate the NLRP3 inflammasome to induce inflammatory responses by mediating immune cell infiltration and aggravating injury [48, 49]. Apelin inhibits the activation of the NLRP3 inflammasome, attenuates the systemic inflammatory response, ameliorates insulin resistance, and promotes survival after severe burn [31]. In the present study, LPS-induced NLRP3 inflammasome activation and enhanced caspase-1 activity were inhibited by apelin; furthermore, the maturation and release of IL-1β in lung tissues were also suppressed by apelin in mice and in Raw264.7 cells.

## Conclusion

In conclusion, the exogenous administration of apelin-13 significantly improved LPS-induced lung injury in mice. A schematic for protective of apelin from LPS-induced lung injury is illustrated in Fig. 7E. Our study implies that apelin-13 may alleviate LPS-induced lung injury by inhibiting oxidative stress damage, cell apoptosis, and NF-κB signaling as well as the NLRP3 inflammasome pathway *in vivo* and *in vitro*. The above evidence provides new targets and new ideas for the diagnosis and treatment of acute lung injury and suggests that apelin-13 should be considered as an agent for the treatment of ALI.

## Abbreviations

LPS (Lipopolysaccharide); NLRs (NOD-like receptors); NLRP3 (NOD-like receptor protein 3); ROS (Reactive oxygen species); TNF-α, Tumor (necrosis factor-α); Caspase-1 (Cysteinyl aspartate specific proteinase-1).

## Acknowledgements

This work was supported by grants from the Zhejiang Provincial Natural Science Funding (LY17H010009, LY17H010005, Y17H160193), the National Science Foundation of China (No. 81772450, No.81472165, No. 81600033).

## Disclosure Statement

The authors declare that there is no conflict of interests associated with this work.

## References

1 Zhang LP, Zhao Y, Liu GJ, Yang DG, Dong YH, Zhou LH: Glabridin attenuates lipopolysaccharide-induced acute lung injury by inhibiting p38MAPK/ERK signaling pathway. Oncotarget 2016;8:18935-18942.
2 Bosmann M, Ward PA: Role of C3, C5 and Anaphylatoxin Receptors in Acute Lung Injury and in Sepsis. Adv Exp Med Biol 2012;946:147-159.

3 Modrykamien AM, Gupta P: The acute respiratory distress syndrome. Proc (Bayl Univ Med Cent) 2015;28:163-171.
4 Bosmann M, Grailer JJ, Russkamp NF, Ruemmler R, Zetoune FS, Sarma JV, Ward PA: CD11c+ alveolar macrophages are a source of IL-23 during lipopolysaccharide-induced acute lung injury. Shock 2013;39:447-452.
5 Park JR, Lee H, Kim SI, Yang SR: The tri-peptide GHK-Cu complex ameliorates lipopolysaccharide-induced acute lung injury in mice. Oncotarget 2016;7:58405-58417.
6 Zeng M, Sang W, Chen S, Chen R, Zhang H, Xue F, Li Z, Liu Y, Gong Y, Zhang H, Kong X: 4-PBA inhibits LPS-induced inflammation through regulating ER stress and autophagy in acute lung injury models. Toxicol Lett 2017;271:26-37.
7 Luo M, Hu L, Li D, Wang Y, He Y, Zhu L, Ren W: MD-2 regulates LPS-induced NLRP3 inflammasome activation and IL-1beta secretion by a MyD88/NF-κB-dependent pathway in alveolar macrophages cell line. Mol Immunol 2017;90:1-10.
8 Zhang Q, Jiang X, He W, Wei K, Sun J, Qin X, Zheng Y, Jiang X: MCL Plays an Anti-Inflammatory Role in Mycobacterium tuberculosis-Induced Immune Response by Inhibiting NF-κB and NLRP3 Inflammasome. Mediators Inflamm 2017;2017:2432904.
9 Wang K, Zhu X, Zhang K, Yao Y, Zhuang M, Tan C, Zhou F, Zhu L: Puerarin inhibits amyloid β-induced NLRP3 inflammasome activation in retinal pigment epithelial cells via suppressing ROS-dependent oxidative and endoplasmic reticulum stresses. Exp Cell Res 2017;357:335-340.
10 Hornung V, Bauernfeind F, Halle A, Samstad EO, Kono H, Rock KL, Fitzgerald KA, Latz E: Silica crystals and aluminum salts activate the NALP3 inflammasome through phagosomal destabilization. Nat Immunol 2008;9:847-856.
11 Kailasan VS, Rathinam VA, Atianand MK, Kalantari P, Skehan B, Fitzgerald KA, Leong JM: Bacterial RNA: DNA hybrids are activators of the NLRP3 inflammasome. Proc Natl Acad Sci USA 2014;111:7765-7770.
12 Rathinam VK, Vanaja SK, Waggoner L, Sokolovska A, Becker C, Stuart LM, Leong JM, Fitzgerald KA: TRIF Licenses Caspase-11-Dependent NLRP3 Inflammasome Activation by Gram-Negative Bacteria. Cell 2012;150:606-619.
13 Willingham SB, Allen IC, Bergstralh DT, Brickey WJ, Huang MT, Taxman DJ, Duncan JA, Ting JP: NLRP3 (NALP3, cryopyrin) facilitates *in vivo* caspase-1, necrosis, & HMGB1 release via inflammasome-dependent and –independent pathways. J Immunol 2009;183:2008-2015.
14 Veerdonk VD, Frank L, Netea MG, Dinarello CA, Joosten LA: Inflammasome activation and IL-1β and IL-18 processing during infection. Trends Immunol 2011;32:110-116.
15 Davis BK, Wen H, and Ting PY: The Inflammasome NLRs in Immunity, Inflammation, and Associated Diseases. Annu Rev Immunol 2011;29:707-735.
16 Bauer C, Duewell P, Mayer C, Lehr HA, Fitzgerald KA, Dauer M, Tschopp J, Endres S, Latz E, Schnurr M: Colitis induced in mice with dextran sulfate sodium (DSS) is mediated by the NLRP3 inflammasome. Gut 2010;59:1192-1199.
17 Wu J, Yan Z, Schwartz DE, Yu J, Malik AB, Hu G: Activation of NLRP3 inflammasome in alveolar macrophages contributes to mechanical stretch-induced lung inflammationand injury. J Immunol 2013;190:3590-3599.
18 Hoegen T, Tremel N, Klein M, Angele B, Wagner H, Kirschning C, Pfister HW, Fontana A, Hammerschmidt S, Koedel U: The NLRP3 inflammasome contributes to brain injury in pneumococcal meningitis and is activated through ATP-dependent lysosomal cathepsin B release. J Immunol 2011;187:5440-5451.
19 Goetze JP, Rehfeld JF, Carlsen J, Videbaek R, Andersen CB, Boesgaard S, Friis-Hansen L: Apelin: A new plasma marker of cardiopulmonary disease. Regul Pept 2006;133:134-138.
20 Habata Y, Fujii R, Hosoya M, Fukusumi S, Kawamata Y, Hinuma S, Kitada C, Nishizawa N, Murosaki S, Kurokawa T, Onda H, Tatemoto K, Fujino M: Apelin, the natural ligand of the orphan receptor APJ, is abundantly secreted in the colostrum. Biochim Biophys Acta 1999;1452:25-35.
21 Kawamata Y, Habata Y, Fukusumi S, Hosoya M, Fujii R, Hinuma S, Nishizawa N, Kitada C, Onda H, Nishimura O, Fujino M: Molecular properties of apelin: tissue distribution and receptor binding. Biochim Biophys Acta 2001;1538:162-171.
22 O'Carroll AM, Selby TL, Palkovits M, Lolait SJ: Distribution of mRNA encoding B78/apj, the rat homologue of the human APJ receptor, and its endogenous ligand apelin in brain and peripheral tissues. Biochim Biophys Acta 2000;1492:72-80.

23 Masri B, Knibiehler B, Audigier Y: Apelin signalling: a promising pathway from cloning to pharmacology. Cell Signal 2005;17:415-426.
24 Kleinz MJ, Davenport AP: Emerging roles of apelin in biology and medicine. Pharmacol Ther 2005;107:198-211.
25 Yang JH, Pan CS, Jia YX, Zhang J, Zhao J, Pang YZ, Yang J, Tang CS, Qi YF: Intermedin1-53 activates L-arginine/nitric oxide synthase/nitric oxide pathway in rat aortas. Peptides 2006;341:567-572.
26 Ladeiras-Lopes R, Ferreira-Martins J, Leite-Moreira AF: The apelinergic system: the role played in human physiology and pathology and potential therapeutic applications. Arq Bras Cardiol 2008;90:343-349.
27 Fukushima H, Kobayashi N, Takeshima H, Koguchi W, Ishimitsu T: Effects of olmesartan on Apelin/APJ and Akt/endothelial nitric oxide synthase pathway in Dahl rats with end-stage heart failure. J Cardiovasc Pharmacol 2010;55:83-88.
28 Falcãopires I, Gonçalves N, Henriques-Coelho T, Moreira-Gonçalves D, Roncon-Albuquerque R Jr, Leite-Moreira AF: Apelin decreases myocardial injury and improves right ventricular function in monocrotaline-induced pulmonary hypertension. Am J Physiol Heart Circ Physiol 2009;296:H2007-H2014.
29 Fan J, Ding L, Xia D, Chen D, Jiang P, Ge W, Zhao R, Guo J, Fan X, Xue F, Wang Y, Mao S, Hu L, Gong Y: Amelioration of apelin-13 in chronic normobaric hypoxia-induced anxiety-like behavior is associated with an inhibition of NF-κB in the hippocampus. Brain Res Bull 2017;130:67-74.
30 Zhang Q, Wu D, Yang Y, Liu T, Liu H：Dexmedetomidine Alleviates Hyperoxia-Induced Acute Lung Injury via Inhibiting NLRP3 Inflammasome Activation. Cell Physiol Biochem 2017;42:1907-1919.
31 Chi Y, Chai J, Xu C, Luo H, Zhang Q: Apelin inhibits the activation of the nucleotide-binding domain and the leucine-rich, repeat-containing family, pyrin-containing 3 (NLRP3) inflammasome and ameliorates insulin resistance in severely burned rats. Surgery 2015;157:1142-1152.
32 Luo Q, Liu G, Chen G, Guo D, Xu L, Hang M, Jin M: Apelin protects against sepsis-induced cardiomyopathy by inhibiting the TLR4 and NLRP3 signaling pathways. Int J Mol Med 2018;42:1161-1167.
33 Kleinz MJ, Davenport AP: Immunocytochemical localization of the endogenous vasoactive peptide apelin to human vascular and endocardial endothelial cells. Regul Pept 2004;118:119-125.
34 Chen MM, Ashley EA, Deng DX, Tsalenko A, Deng A, Tabibiazar R, Ben-Dor A, Fenster B, Yang E, King JY, Fowler M, Robbins R, Johnson FL, Bruhn L, McDonagh T, Dargie H, Yakhini Z, Tsao PS, Quertermous T: Novel Role for the Potent Endogenous Inotrope Apelin in Human Cardiac Dysfunction. Circulation 2003;108:1432-1439.
35 Szokodi I, Tavi P, Földes G, Voutilainen-Myllylä S, Ilves M, Tokola H, Pikkarainen S, Piuhola J, Rysä J, Tóth M, Ruskoaho H: Apelin, the novel endogenous ligand of the orphan receptor APJ, regulates cardiac contractility. Circ Res 2002;91:434-440.
36 Berry MF, Pirolli TJ, Jayasankar V, Burdick J, Morine KJ, Gardner TJ, Woo YJ: Apelin has *in vivo* inotropic effects on normal and failing hearts. Circulation 2004;110:187-193.
37 Ashley EA, Powers J, Chen M, Kundu R, Finsterbach T, Caffarelli A, Deng A, Eichhorn J, Mahajan R, Agrawal R, Greve J, Robbins R, Patterson AJ, Bernstein D, Quertermous T: The endogenous peptide apelin potently improves cardiac contractility and reduces cardiac loading *in vivo*. Cardiovasc Res 2005;65:73-82.
38 Fan XF, Xue F, Zhang YQ, Xing XP, Liu H, Mao SZ, Kong XX, Gao YQ, Liu SF, Gong YS: The Apelin-APJ axis is an endogenous counterinjury mechanism in experimental acute lung injury. Chest 2015;147:969-978.
39 Kellner M, Noonepalle S, Lu Q, Srivastava A, Zemskov E, Black SM: ROS Signaling in the Pathogenesis of Acute Lung Injury (ALI) and Acute Respiratory Distress Syndrome (ARDS). Adv Exp Med Biol 2017;967:105-137.
40 Zhang Z, Yu B, Tao GZ: Apelin protects against cardiomyocyte apoptosis induced by glucose deprivation. Chin Med J (Engl) 2009;122:2360-2365.
41 Simpkin JC, Yellon DM, Davidson SM, Lim SY, Wynne AM, Smith CC: Apelin-13 and apelin-36 exhibit direct cardioprotective activity against ischemiareperfusion injury. Basic Res Cardiol 2007;102:518-528.
42 Foussal C, Lairez O, Calise D, Pathak A, Guilbeau-Frugier C, Valet P, Parini A, Kunduzova O: Activation of catalase by apelin prevents oxidative stress - linked cardiac hypertrophy. Febs Lett 2010;584:2363-2370.
43 Matutebello G, Frevert CW, Martin TR: Animal models of acute lung injury. Am J Physiol Lung Cell Mol Physiol 2008;295:379-399.
44 Grommes J, Soehnlein O: Contribution of neutrophils to acute lung injury. Mol Med 2011;17:293-307.

45 Chung IS, Kim JA, Kim JA, Choi HS, Lee JJ, Yang M, Ahn HJ, Lee SM: Reactive oxygen species by isoflurane mediates inhibition of nuclear factor κB activation in lipopolysaccharide-induced acute inflammation of the lung. Anesth Analg 2013;116:327-335.

46 Cho RL, Yang CC, Lee IT, Lin CC, Chi PL, Hsiao LD, Yang CM: Lipopolysaccharide induces ICAM-1 expression via a c-Src/NADPH oxidase/ROS-dependent NF-κB pathway in human pulmonary alveolar epithelial cells. Am J Physiol Lung Cell Mol Physiol 2016;310:L639-657.

47 Lu Y, Zhu X, Liang GX, Cui RR, Liu Y, Wu SS, Liang QH, Liu GY, Jiang Y, Liao XB, Xie H, Zhou HD, Wu XP, Yuan LQ, Liao EY: Apelin-APJ induces ICAM-1, VCAM-1 and MCP-1 expression via NF-κB/JNK signal pathway in human umbilical vein endothelial cells. Amino Acids 2012;43:2125-2136.

48 Mao K, Chen S, Chen M, Ma Y, Wang Y, Huang B, He Z, Zeng Y, Hu Y, Sun S, Li J, Wu X, Wang X, Strober W, Chen C, Meng G, Sun B: Nitric oxide suppresses NLRP3 inflammasome activation and protects against LPS-induced septic shock. Cell Res 2013;23:201-212.

49 Baker PJ, Boucher D, Bierschenk D, Tebartz C, Whitney PG, D'Silva DB, Tanzer MC, Monteleone M, Robertson AA, Cooper MA, Alvarez-Diaz S, Herold MJ, Bedoui S, Schroder K, Masters SL: NLRP3 inflammasome activation downstream of cytoplasmic LPS recognition by both caspase-4 and caspase-5. Eur J Immunol 2015;45:2918-2926.